Discovery of a selective $Na_V1.7$ inhibitor from centipede venom with analgesic efficacy exceeding morphine in rodent pain models

Shilong Yang[a,b,1], Yao Xiao[a,b,1], Di Kang[a,b,1], Jie Liu[a,b], Yuan Li[a,b], Eivind A. B. Undheim[c], Julie K. Klint[c], Mingqiang Rong[a,2], Ren Lai[a,2], and Glenn F. King[c,2]

[a]Key Laboratory of Animal Models and Human Disease Mechanisms, Kunming Institute of Zoology, Chinese Academy of Sciences and Yunnan Province, Kunming 650223, Yunnan, China; [b]Graduate School of Chinese Academy of Sciences, Beijing 100009, China; and [c]Division of Chemistry and Structural Biology, Institute for Molecular Bioscience, The University of Queensland, St. Lucia, QLD 4072, Australia

Edited* by Baldomero M. Olivera, University of Utah, Salt Lake City, UT, and approved September 4, 2013 (received for review April 3, 2013)

Loss-of-function mutations in the human voltage-gated sodium channel $Na_V1.7$ result in a congenital indifference to pain. Selective inhibitors of $Na_V1.7$ are therefore likely to be powerful analgesics for treating a broad range of pain conditions. Herein we describe the identification of μ-SLPTX-Ssm6a, a unique 46-residue peptide from centipede venom that potently inhibits $Na_V1.7$ with an IC_{50} of ∼25 nM. μ-SLPTX-Ssm6a has more than 150-fold selectivity for $Na_V1.7$ over all other human Na_V subtypes, with the exception of $Na_V1.2$, for which the selectivity is 32-fold. μ-SLPTX-Ssm6a contains three disulfide bonds with a unique connectivity pattern, and it has no significant sequence homology with any previously characterized peptide or protein. μ-SLPTX-Ssm6a proved to be a more potent analgesic than morphine in a rodent model of chemical-induced pain, and it was equipotent with morphine in rodent models of thermal and acid-induced pain. This study establishes μ-SPTX-Ssm6a as a promising lead molecule for the development of novel analgesics targeting $Na_V1.7$, which might be suitable for treating a wide range of human pain pathologies.

chronic pain | drug discovery | peptide therapeutic

Normal pain is a key adaptive response that serves to limit our exposure to potentially damaging or life-threatening events. In contrast, aberrant long-lasting pain transforms this adaptive response into a debilitating and often poorly managed disease. Chronic pain affects ∼20% of the population, with the incidence rising significantly in elderly cohorts (1). The economic burden of chronic pain in the United States was recently estimated to be ∼$600 billion per annum, which exceeds the combined annual cost of cancer, heart disease, and diabetes (2). There are few drugs available for treatment of chronic pain, and many of these have limited efficacy and dose-limiting side-effects.

Voltage-gated sodium (Na_V) channels are integral transmembrane proteins that provide a current pathway for the rapid depolarization of excitable cells (1, 3), and they play a key role in conveying nociceptor responses to synapses in the dorsal horn (4). Humans contain nine different Na_V channel subtypes, denoted $Na_V1.1$ to $Na_V1.9$ (5, 6). In recent years, $Na_V1.7$ has emerged as a promising analgesic target based on several remarkable human genetic studies. Gain-of-function mutations in the *SNC9A* gene encoding the pore-forming α-subunit of $Na_V1.7$ cause severe episodic pain in inherited neuropathies, such as erythromelalgia and paroxysmal extreme pain disorder (7), whereas loss-of-function mutations in *SCN9A* result in a congenital indifference to pain (CIP) (8). The latter phenotype can be recapitulated in rodents via complete knockout of $Na_V1.7$ in all sensory and sympathetic neurons (9). Moreover, certain polymorphisms in *SCN9A* correlate with sensitivity to nociceptive inputs (10). Remarkably, apart from their inability to sense pain, loss of smell (anosmia) is the only other sensory impairment in individuals with CIP (11, 12). Thus, the combined genetic data suggest that subtype-selective blockers of $Na_V1.7$ are likely to be useful analgesics for treating a broad range of pain conditions.

Centipedes are one of the oldest extant arthropods, with the fossil record dating back 430 million y (13). Centipedes were one of the first terrestrial taxa to use venom as a predation strategy, and they have adapted to capture a wide variety of prey, including insects, fish, molluscs, amphibians, reptiles, and even mammals (13, 14). The centipede venom apparatus, which is unique and bears little resemblance to that of other arthropods, evolved by modification of the first pair of walking legs into a set of pincer-like claws (forcipules) (13). Venom is secreted via a pore located near the tip of each forcipule. There are ∼3,300 extant species of centipedes, yet the venom of only a handful has been studied in any detail. We recently demonstrated that the venom of the Chinese red-headed centipede *Scolopendra subspinipes mutilans* is replete with unique, disulfide-rich peptides that potently modulate the activity of mammalian voltage-gated ion channels (14), and therefore we decided to explore this venom as a potential source of $Na_V1.7$ inhibitors. We describe the purification from this venom of a highly selective inhibitor of $Na_V1.7$ that is a more effective analgesic than morphine in rodent pain models.

Results

Purification of μ-SLPTX-Ssm6a. A unique peptide denoted μ-SLPTX-Ssm6a (hereafter Ssm6a) was purified from venom of the centipede *S. subspinipes mutilans* using a combination of Sephadex G-50 gel-

Significance

The economic burden of chronic pain in the United States is currently ∼$600 billion per annum, which exceeds the combined annual cost of cancer, heart disease, and diabetes. Few drugs are available for treating chronic pain, and many have limited efficacy and dose-limiting side-effects. Humans with inheritable loss-of-function mutations in the voltage-gated sodium channel $Na_V1.7$ are indifferent to all types of pain, and therefore drugs that block this channel should be useful analgesics for treating many pain conditions. Herein we describe Ssm6a, a peptide from centipede venom that potently and selectively blocks the human $Na_V1.7$ channel. Ssm6a proved to be more analgesic than morphine in rodent pain models and did not cause any side-effects.

Author contributions: M.R., R.L., and G.F.K. designed research; S.Y., Y.X., D.K., J.L., Y.L., E.A.B.U., and J.K.K. performed research; S.Y., Y.X., D.K., J.L., Y.L., E.A.B.U., J.K.K., M.R., R.L., and G.F.K. analyzed data; and S.Y., M.R., R.L., and G.F.K. wrote the paper.

The authors declare no conflict of interest.

*This Direct Submission article had a prearranged editor.

[1]S.Y., Y.X., and D.K. contributed equally to this work.

[2]To whom correspondence may be addressed. E-mail: rongmingqiang@mail.kiz.ac.cn, rlai@mail.kiz.ac.cn, or glenn.king@imb.uq.edu.au.

This article contains supporting information online at www.pnas.org/lookup/suppl/doi:10.1073/pnas.1306285110/-/DCSupplemental.

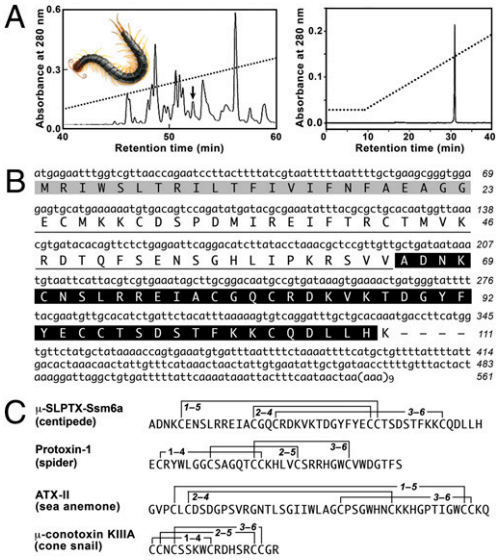

Fig. 1. Purification of Ssm6a from venom of the centipede *S. subspinipes mutilans*. (*A*) Lyophilized venom (2.0 mg) was dissolved in 0.1 M phosphate, pH 6.0 then fractionated on a C_{18} RP-HPLC column (*Left*). Elution was performed at a flow rate of 1.5 mL/min using a gradient of acetonitrile in 0.1% trifluoroacetic acid. The peak indicated by an arrow was purified further by analytical C_{18} RP-HPLC (*Right*) using a shallower acetonitrile gradient. (*Inset*) A photo by Yasunori Koide of *S. subspinipes mutilans*. (*B*) Sequence of transcript encoding Ssm6a. The signal peptide is shown in gray, the propeptide region is underlined, and the mature peptide is shown with white text on a black background. The 3′-UTR including the poly(A) tail is also shown. (*C*) Comparison of the primary structure of Ssm6a with other venom peptides reported to act on $Na_V1.7$, including protoxin-1 (27), ATX-II (39), and μ-conotoxin KIIIA (40).

filtration chromatography and reverse-phase (RP) HPLC (Fig. 1*A*). The primary structure of Ssm6a was determined via Edman degradation in combination with analysis of a venom-gland transcriptome (Fig. 1*B*). The 46-residue mature toxin is produced by posttranslational processing of a 111-residue prepropeptide (Fig. 1*B*), its mass determined using MALDI-TOF mass spectrometry (5318.4 Da) (Fig. S1) indicates that the six cysteine residues form three disulfide bonds. A BLAST search of the protein/DNA sequence databases revealed that Ssm6a is not similar to any known peptide or protein, except for ∼40% sequence identity with κ-SLPTX-Ssm1a that we recently isolated from the venom of the same centipede (14).

Partial reduction of native Ssm6a with Tris (2-carboxyethyl) phosphine (TCEP) yielded four peaks when the sample was fractionated using RP-HPLC (Fig. S2). The mass of peaks II and III were increased by 2 Da and 4 Da, respectively, relative to the native peptide indicating that they contained either one (peak II) or two (peak III) reduced disulfide bonds (Fig. S2). These partially reduced peptides were alkylated with iodoacetamide then subjected to Edman degradation. Peak II yielded alkylated Cys residues in cycles 5 and 32 (Fig. S3), indicative of a Cys5–Cys32 disulfide bridge in the native toxin. Sequencing of peak III was inconclusive. Analysis of side-chain/side-chain dipolar connectivities (15) in a 2D ^1H-^1H NOESY spectrum of Ssm6a revealed that the remaining two disulfide bridges are Cys15–Cys31 and Cys18–Cys41 (Fig. 1*C*).

Effect of μ-SLPTX-Ssm6a on Na_V Channels. Because $Na_V1.7$ is preferentially expressed in dorsal root ganglia (DRG) and sympathetic neurons (16), we investigated the ability of Ssm6a to block $Na_V1.7$ channel currents in adult rat DRG neurons using whole-cell patch-clamp electrophysiology. Although $Na_V1.7$ is the most highly expressed Na_V channel in DRG neurons, they also express other subtypes, including $Na_V1.8$ and $Na_V1.9$.

Cells were held at –80 mV for over 5 min to allow adequate equilibration, then current traces were evoked using a 50-ms step depolarization to –10 mV every second. TTX (100 nM) was added to the bathing solution to separate TTX-resistant (TTX-r) currents from other sodium currents in DRG neurons (17). $Na_V1.5$, $Na_V1.8$, and $Na_V1.9$ are TTX-r, whereas all other subtypes are TTX-sensitive (TTX-s). TTX-s currents were completely inhibited by 1 μM Ssm6a, whereas 10 μM toxin had no effect on TTX-r currents (Fig. 2*A*). Inhibition of TTX-s currents was dose-dependent with an IC_{50} of 23 nM (Fig. 2*B*). The action of Ssm6a on TTX-s currents was fast, and toxin dissociation was rapid after washing with extracellular solution. Time constants governing block (τ_{on}) and unblock (τ_{off}) following exposure to 1 μM Ssm6a were 8.0 s and 10.2 s, respectively.

In the presence of 20 nM Ssm6a, the current–voltage relationship for TTX-s Na_V channel currents was shifted ∼15 mV in a depolarizing direction (Fig. 2*D*), and consequently the channel conductance–voltage relationship was positively shifted by ∼18 mV (Fig. 2*E*). In contrast, Ssm6a did not induce a shift in steady-state inactivation of TTX-s Na_V channel currents in DRG neurons (Fig. 2*F*). At a saturating concentration of Ssm6a (1 μM), the inhibition of TTX-s currents in rat DRG neurons and HEK293 cells expressing human $Na_V1.7$ was partly overcome by depolarizations to large positive test potentials (>60 mV) (Fig. S4). This partial reversal of channel inhibition, along with the depolarizing shift in the voltage dependence of activation, is characteristic of gating modifiers that interact with the voltage-sensing domains of Na_V channels (18). In contrast, as expected, inhibition of $Na_V1.7$ currents by the pore-blocker TTX was largely voltage-independent (Fig. S4).

Selectivity of Ssm6a for Na_V Channel Subtypes. We examined the effect of Ssm6a on human (h) Na_V channel subtypes 1.1–1.8 expressed in HEK293 cells. Currents were elicited by a 20-ms

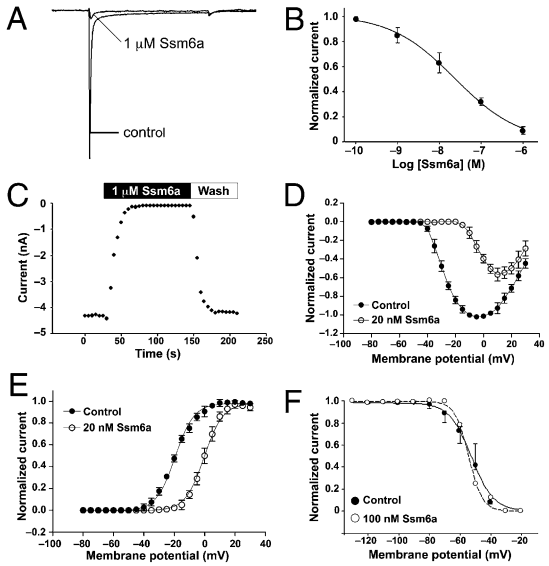

Fig. 2. Effect of Ssm6a on Na_V channel currents in rat DRG neurons. All current traces were evoked by a 50-ms step depolarization to –10 mV from a holding potential of –80 mV every 5 s. (*A*) Inhibition of TTX-s Na_V channel currents by 1 μM Ssm6a. (*B*) Concentration–response curve for block of TTX-s Na_V currents in DRG neurons by Ssm6a ($n = 5$). (*C*) Time course for block of TTX-s currents by Ssm6a and reversal of block by washing with external solution. (*D*) Current–voltage (I–V) relationship for TTX-s currents before and after application of 100 nM Ssm6a. (*E*) Ssm6a shifts the conductance–voltage relationship to more positive potentials ($n = 5$). (*F*) Ssm6a had no effect on the voltage-dependence of steady-state inactivation, which was estimated using a standard double-pulse protocol ($n = 5$). Data points are expressed as mean ± SE and curves are fits to either the Hill (*B*, *D*, *E*) or Boltzmann (*F*) equation.

depolarizing potential of –10 mV from a holding potential of –80 mV every 5 s. At a concentration of 50 nM, Ssm6a potently inhibited $hNa_V1.7$, decreasing current amplitude by ~63% (Fig. 3*D*). The peptide was a much weaker inhibitor of $hNa_V1.1$, $hNa_V1.2$, and $hNa_V1.6$; at 2 μM, Ssm6a depressed $hNa_V1.1$ currents ~by 25% (Fig. 3*A*), whereas 1 μM Ssm6a reduced $hNa_V1.2$ and $hNa_V1.6$ currents by 31% (Fig. 3*B*) and 25% (Fig. 3*C*), respectively. The calculated IC_{50} values were 4.1 μM, 813 nM, 15.2 μM, and 25.4 nM for $hNa_V1.1$, $hNa_V1.2$, $hNa_V1.6$, and $hNa_V1.7$, respectively (Fig. 3*E*). Ssm6a had no effect on $hNa_V1.3$, $hNa_V1.4$, $hNa_V1.5$, and $hNa_V1.8$ (Fig. S5).

Similar to the effect of protoxin-II on rat DRG neurons, Ssm6a shifted the conductance–voltage relationship in a depolarizing direction (19). Ssm6a shifted the conductance–voltage relationship about +10.7, +12.9, +9.55, and +13.5 mV for $hNa_V1.1$, $hNa_V1.2$, $hNa_V1.6$, and $hNa_V1.7$, respectively (Fig. 4). Ssm6a did not induce a shift in steady-state inactivation for these Na_V channel subtypes (Fig. 4).

Notably, the concentration–response curves for Ssm6a inhibition of TTX-s Na_V currents in DRG neurons (Fig. 2*B*) and $hNa_V1.7$ currents in HEK293 cells (Fig. 3*E*) were rather shallow (Hill coefficient ~0.5), suggesting that the peptide might interact with multiple sites on $Na_V1.7$ that exhibit negative cooperativity. Such a mechanism of action would not be unprecedented, because it has been demonstrated that several Na_V channel toxins derived from arachnid venoms bind to more than one of the voltage-sensor paddles in $Na_V1.2$ (19).

Effects of Ssm6a on Pain. Because $Na_V1.7$ plays a key role in nociception in humans, the analgesic effect of Ssm6a was tested in several rodent pain models in which pain was induced by noxious chemicals, acid, or heat.

Intraplantar injection of formalin leads to a biphasic pain response in mice: an early nociceptive response (phase I, 0–5 min) caused by direct stimulation of TRPA1 in a subpopulation of C-fiber nociceptors is followed by a quiescent period that precedes a second phase of nociceptive behavior (phase II, 15–30 min) because of peripheral inflammation together with central sensitization (20). Intraperitoneal injection of Ssm6a drastically decreased both phase I and phase II responses (Fig. 5*A*). Control mice (saline injection) licked their paws an average of 212 times during phase I. Ssm6a was highly effective at attenuating phase I pain, with the number of paw licks reduced by 14%, 60%, and 92% at peptide concentrations of 1, 10, and 100 nmol/kg, respectively (Fig. 5*A*). On a molar basis, Ssm6a was significantly more effective than morphine, which reduced the number of paw licks during phase I by 3%, 19%, and 69% at concentrations of 1, 10, and 100 nmol/kg, respectively (Fig. 5*A*).

Ssm6a was also highly effective at attenuating the second phase of nociceptive behavior following formalin injection, during which control mice licked their paws an average of 694 times. At concentrations of 1, 10, and 100 nmol/kg, Ssm6a decreased the number of paw licks during phase II by 25%, 54%, and 80%, respectively (Fig. 5*B*). On a molar basis, Ssm6a was significantly more effective than morphine, which reduced the number of paw licks during phase II by 3%, 16%, and 57% at concentrations of 1, 10, and 100 nmol/kg, respectively (Fig. 5*B*).

Ssm6a was as effective as morphine in reducing abdominal writhing induced in mice by intraperitoneal injection of acid (Fig. 5*C*). At concentrations of 1, 10, and 100 nmol/kg, Ssm6a decreased the number of writhing movements by 29%, 51%, and 79%, respectively (Fig. 5*C*), which is similar to the reductions of 25%, 44%, and 76% caused by equivalent concentrations of morphine (Fig. 5*C*).

Ssm6a and morphine were similarly effective at reducing thermal pain (Fig. 5*D*). In mice subjected to photothermal heat, tail withdrawal latency was increased from 5 s in the saline-treated control group to 6.3 s, 9.2 s, and 13.4 s in mice treated with 1, 10, and 100 nmol/kg Ssm6a, respectively. Similar increases in paw withdrawal latency were observed for mice treated with the same concentrations of morphine (Fig. 5*D*).

Side-Effect Profile. At doses up to 10-fold higher than those for which we observed robust analgesic effects, Ssm6a had no evident side effects. At a dose of 1 μmol/kg, Ssm6a had no effect on blood pressure (Fig. S6*A*), heart rate (Fig. S6*B*), or motor function (Fig. S6*C*).

Plasma Stability and Duration of Action of Ssm6a. Ssm6a must be highly stable in vivo because it drastically reduced nociceptive behavior in phase II of the formalin-induced pain model, the onset of which occurred ~45 min after intraperitoneal injection of the peptide. Consistent with this hypothesis, Ssm6a was found to be extraordinarily stable in isolated human plasma, with no significant degradation over 1 wk, compared with a half-life of 64 min for rat atrial natriuretic peptide under the same conditions (Fig. 6*A*). However, the analgesic effect of Ssm6a declined monotonically over a period of 4 h in rodent models of acid- and heat-induced pain, as well as phase I of the formalin pain model. Interestingly, at the highest doses tested, Ssm6a still produced robust analgesic effects after 4 h in phase II of the formalin pain model. The major factor determining systemic concentrations of Ssm6a, and thus the time course of its analgesic efficacy, is likely to be the rate at which it is cleared by the liver and kidney (21).

Because of its unique amino acid sequence and disulfide framework, we propose that Ssm6a has a unique 3D structure. Consistent with this hypothesis, the far-UV CD spectrum of Ssm6a (Fig. 6*B*) revealed that it is predominantly α-helical, in striking contrast to all other venom peptides that target Na_V channels whose primary secondary structure elements are two to three β-strands. This unusual 3D-fold not only provides Ssm6a with a high level of resistance to proteases, as evidenced by its stability in human plasma, but it also provides it with unusually high thermal stability. We were unable to obtain complete thermal unfolding curves for Ssm6a in the absence of a chemical denaturant; even in 4 M urea, the peptide was only ~50% unfolded at 90 °C (Fig. 6*C*). The estimated midpoint (T_m) of the

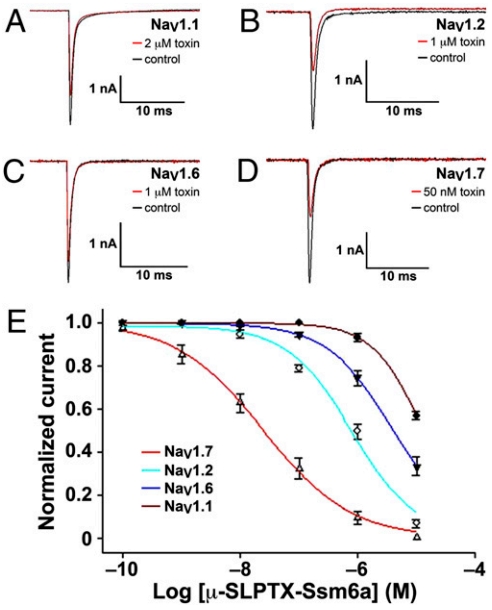

Fig. 3. Effect of Ssm6a on $hNa_V1.1$, $hNa_V1.2$, $hNa_V1.6$, and $hNa_V1.7$ expressed in HEK293 cells. Current traces were evoked by a 50-ms step depolarization to −10 mV from a holding potential of −80 mV every 5 s. Control currents are shown in black and current traces showing inhibition of $hNa_V1.1$ (*A*), $hNa_V1.2$ (*B*), $hNa_V1.6$ (*C*), and $hNa_V1.7$ (*D*) by the indicated concentrations of Ssm6a are shown in red. (*E*) Concentration-response curves for inhibition of $hNa_V1.1$, $hNa_V1.2$, $hNa_V1.6$, and $hNa_V1.7$ by Ssm6a (n = 5).

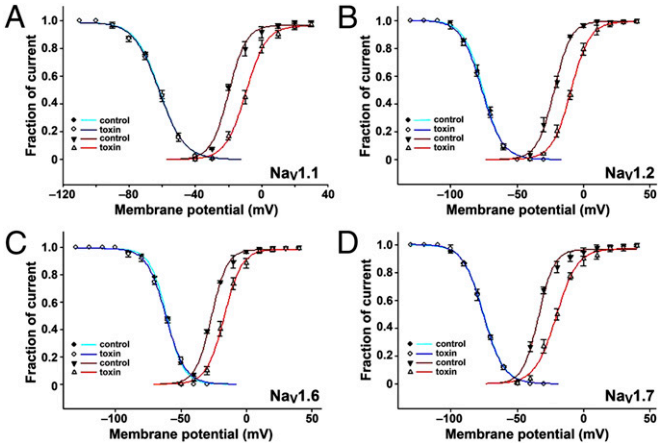

Fig. 4. Effect of Ssm6a on current-voltage relationships. Ssm6a induced a depolarizing shift in the I-V curves for activation of (*A*) $hNa_V1.1$ (10.7-mV shift at 10 μM), (*B*) $hNa_V1.2$ (12.9-mV shift at 1 μM), (*C*) hNav1.6 (9.5-mV shift at 5 μM), and (*D*) hNav1.7 (13.5-mV shift at 20 nM). In contrast, the peptide had no effect on steady-state inactivation of these channels (*A*–*D*).

thermal unfolding transition for Ssm6a in 8 M urea was 70.6 ± 0.1 °C (Fig. 6*C*).

Discussion

Clinical genetic studies have identified $hNa_V1.7$ as a critical mediator of pain sensitization (7). Loss-of-function mutations in $hNa_V1.7$ cause a congenital indifference to pain with no other sensory impairments except anosmia (8, 22, 23), whereas gain-of-function mutations are associated with painful neuropathies (7, 24). Ablation of $Na_V1.7$ in all mouse sensory neurons abolishes mechanical pain, inflammatory pain, and reflex withdrawal responses to heat, without affecting neuropathic pain. However, ablation of $Na_V1.7$ in both sensory and sympathetic neurons abolishes all pain sensations and recapitulates the pain-free phenotype seen in CIP patients (9). Thus, $Na_V1.7$ appears to be an attractive target for the development of novel analgesics for treating a wide range of pain pathologies.

Development of $Na_V1.7$-based analgesics has proved difficult, as it is essential to avoid off-target effects on closely related Na_V channels with critical physiological roles. In particular, it is essential to avoid off-target effects on $hNa_V1.5$, which is responsible for the rising phase of the cardiac action potential (25), the muscle-specific $hNa_V1.4$, and $hNa_V1.6$, the primary Na_V channel at nodes of Ranvier (26).

Spider venoms have proved to be a rich source of $Na_V1.7$ channel inhibitors (27), but most spider-venom peptides isolated to date are not sufficiently selective to be therapeutically useful. For example, although protoxin-II blocks $hNa_V1.7$ with extremely high affinity (IC_{50} ~300 pM), it is also a high-affinity inhibitor of $hNa_V1.2$ (IC_{50} ~41 nM), $hNa_V1.5$ (IC_{50} ~79 nM), and $hNa_V1.6$ (IC_{50} ~26 nM) (27). Because of its lack of selectivity, protoxin-II proved lethal to rats when administered intravenously at a dose of 1.0 mg/kg or intrathecally at 0.1 mg/kg (28). Although several small-molecule blockers of $hNa_V1.7$ have been described, they generally suffer from a similar lack of subtype selectivity (25, 29).

In this study we examined centipede venom as a potential source of selective $Na_V1.7$ inhibitors because we previously demonstrated that these venoms are replete with ion channel modulators (14). We described the purification and functional characterization of a unique peptide (Ssm6a) with potent analgesic properties from venom of the centipede *S. subspinipes mutilans*. Ssm6a contains 46-residues with three disulfide bonds and it has no significant homology with any previously described protein or peptide. The disulfide linkage pattern (C1–C5, C2–C4, C3–C6) is notably to different to that of the inhibitor cystine knot motif (C1–C4, C2–C5, C3–C6) found in most spider-venom peptides that modulate Na_V channels (27) (Fig. 1*C*). Moreover, Ssm6a is predominantly α-helical, in striking contrast to other venom peptides that target Na_V channels. Despite its unique 3D architecture, both the thermal stability and protease resistance of Ssm6a are reminiscent of spider-venom inhibitor cystine knot peptides (30).

Ssm6a is the most subtype-selective inhibitor of $Na_V1.7$ reported to date. Ssm6a selectively inhibits $hNa_V1.7$ with an IC_{50} of 25 nM (Fig. 3 *D* and *E*) by shifting the voltage-dependence of activation to more depolarized potentials (Fig. 4*D*), but it has no effect on $hNa_V1.3$, $hNa_V1.4$, $hNa_V1.5$, and $hNa_V1.8$, and only inhibits $hNa_V1.1$, $hNa_V1.2$, and $hNa_V1.6$ at very high concentrations. Most importantly from a therapeutic perspective, Ssm6a has 600-fold or higher selectivity for $Na_V1.7$ over the key off-target subtypes $Na_V1.4$, $Na_V1.5$, and $Na_V1.6$, and it has no effect on hERG ($K_V11.1$) at concentrations up to 10 μM (Fig. S7).

Consistent with its potent and highly selective block of $Na_V1.7$, Ssm6a proved to be an effective analgesic in rodent pain models (Fig. 5). On a molar basis, Ssm6a was several-fold more effective than morphine in a rodent model of formalin-induced pain (Fig. 5 *A* and *B*) and it was equipotent with morphine in its ability to reduce thermal and acid-induced pain (Fig. 5 *C* and *D*). Ssm6a is highly stable in human plasma, and intraperitoneal administration of the peptide at doses up to 1 μmol/kg produced no adverse effects on blood pressure, heart rate, or motor function. Thus, Ssm6a appears to be an excellent lead molecule for development of analgesics targeted against $hNa_V1.7$. However, future experiments should be directed toward examination of the analgesic activity of Ssm6a in more complex rodent pain models that better resemble human pain phenotypes, as well as a more detailed assessment of its selectivity for the nociceptive circuitry.

Finally, we speculate that the biological role of Ssm6a in centipede venom is likely to be block of Na_V channels in insect

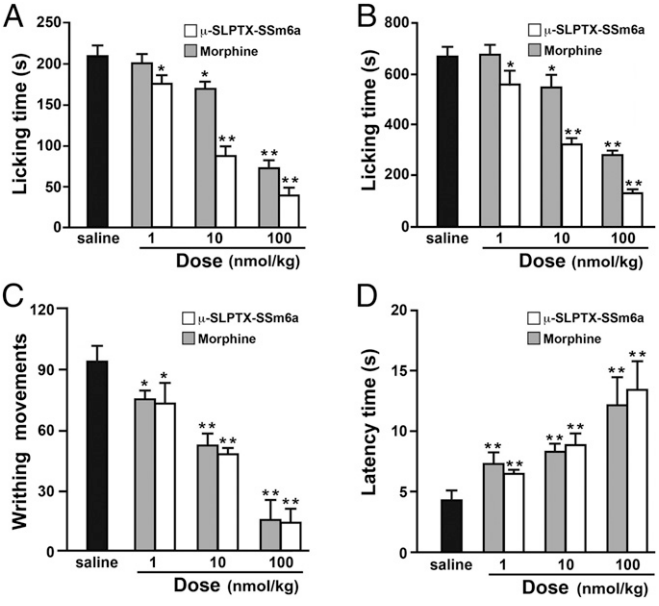

Fig. 5. Analgesic effects of Ssm6a in mice. Ssm6a was more effective than morphine in attenuating nociceptive behavior (paw licking) during (*A*) phase I (0–5 min postinjection) and (*B*) phase II (15–30 min postinjection) following intraplantar injection of formalin. (*C*) Ssm6a and morphine were equally effectively in reducing the abdominal writhing induced by intraperitoneal injection of acetic acid. (*D*) Ssm6a and morphine were equally effectively in increasing the photothermal pain threshold in mice subjected to tail heating. Data points are mean ± SEM (n = 10). Statistically significant differences compared with the saline control group (calculated using a Student t test) are indicated by $^*P<0.05$ and $^{**}P<0.01$.

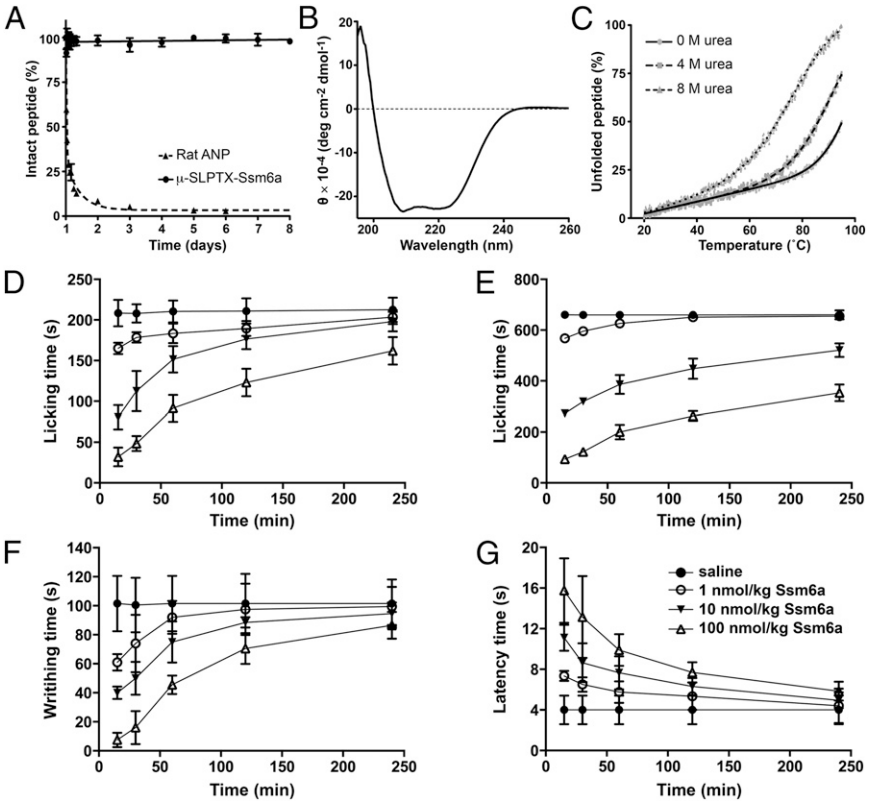

Fig. 6. (*A*) Comparison of the stability of Ssm6a (●) and rat atrial natriuretic peptide in human plasma (▲). Datapoints are mean ± SD (n = 3). (*B*) Far-UV CD spectrum of Ssm6a showing minima characteristic of α-helical secondary structure at 208 and 222 nm. The helical content derived from θ_{222} is 63%. (*C*) Thermal denaturation profile of Ssm6a in 0 (●), 4 (■), and 8 M (▲) urea. Solid lines are fits of a sigmoidal function to the data to obtain T_m values. (*D*–*G*) The duration of the analgesic effects of Ssm6a was determined by monitoring paw licking time during phase I (*D*) and phase II (*E*) in the formalin pain model, writhing movements during acid-induced pain (*F*), and tail withdrawal latency in the thermal pain model (*G*).

prey. In contrast to humans, insects express only a single Na_V channel that is a common target of peptides in the venom of arthropod predators, such as spiders and scorpions (6). Ssm6a blocks hNav.1.7 within seconds of administration (Fig. 2*C*), and a similarly rapid block of insect Na_V channels would induce rapid paralysis and ultimately death of insect prey. The species from which Ssm6a was purified belongs to Scolopendromorpha, one of the five extant orders of centipedes (13), and thus it will be interesting from a toxinological perspective to determine whether this unusual class of toxins is unique to this order or represents a more basal recruitment within the centipede phylogenetic tree.

Although it might seem counterintuitive that a venom peptide used for predation could be a useful therapeutic, the significant differences in primary structure and tissue distribution between insect and human ion channels makes this possible. There are now six Food and Drug Administration-approved drugs derived from venom peptides or proteins, with many more in clinical trials or various stages of preclinical development (21). The approved group includes Prialt, a $Ca_V2.2$ blocker from the venom of a marine cone snail that is used for treatment of severe intractable pain (21). The present study suggests that centipede venoms, which to date have been largely neglected, might provide a novel source of lead molecules for drug development.

Materials and Methods

Assignment of the Disulfide Bonds. Ssm6a (0.1 mg) was partially reduced in 10 μL of citrate buffer (1 M, pH 3.0) containing 6 M guanidine·HCl and 0.05 M TCEP for 10 min at 40 °C. The partially reduced sample was fractionated via C_{18} RP-HPLC using a linear acetonitrile gradient (0–60% over 40 min). Intermediates with free thiols (as determined using MALDI-TOF mass spectrometry) were lyophilized and alkylated with iodoacetamide (0.5 M, pH 8.3). Alkylated peptides were desalted using C_{18} RP-HPLC then subjected to Edman degradation on a Shimadzu protein sequencer (PPSQ-31A; Shimadzu).

Patch-Clamp Recording on Rat DRG Neurons. Rat DRG neurons were acutely dissociated and maintained in short-term primary culture, as previously described (31). Ca^{2+}, Na^+, and K^+ currents were recorded using the whole-cell patch-clamp technique with an Axon Multiclamp 700B amplifier (Molecular Devices). The P/4 protocol was used to subtract linear capacitive and leakage currents. Series resistance was typically 6–8 mΩ and was compensated to 80% (32). Data were acquired and analyzed using Clampfit 10.0 (Molecular Devices) and SigmaPlot (Systat Software). All animal experiments described in this work were approved by the Animal Care and Use Committee at Kunming Institute of Zoology, Chinese Academy of Sciences (2011-162).

Patch-Clamp Recordings on Human Na_V Channels. Human Na_V1 α-subunits, the human $Na_V\beta1$ subunit, and eGFP were transiently transfected into HEK293T cells and whole-cell patch-clamp recordings performed as previously described (33). The standard pipette solution contained: 140 mM CsF, 1 mM EGTA, 10 mM NaCl, 3 mM KCl, and 10 mM $MgCl_2$, pH 7.3. The standard bath solution was: 140 mM NaCl, 3 mM KCl, 1 mM $MgCl_2$, 1 mM $CaCl_2$, and 10 mM Hepes, pH 7.3. Data were acquired and analyzed using Clampfit 10.0 and SigmaPlot. All datapoints are shown as mean ± SE (n = number of separate experimental cells examined). Dose–response curves were fitted using the following Hill logistic equation: $y = 1 - (1 - f_{max})/[1+([Tx]/IC_{50})^n]$ where n is an empirical Hill coefficient and f_{max} is the fraction of current resistant to inhibition at high toxin (Tx) concentration. Steady-state activation and inactivation curves were fitted using the Boltzmann equation: $y = 1/(1 + \exp[(V_{1/2} - V)/k])$ in which $V_{1/2}$, V, and k represented midpoint voltage of kinetics, test potential and slope factor, respectively. τ_{on} and τ_{off} values were obtained from single exponential fits using the equations $I(t) = a_0 + a_1[1 - \exp(-t/\tau_{on})]$ and $I(t) = a_0 + a_1 \exp(-t/\tau_{off})$, respectively.

Formalin-Induced Paw Licking. Pain was induced in mice by intraplantar injection of formalin, and pain attenuation was compared in mice injected intraperitoneally with either morphine or Ssm6a dissolved in 100 μL saline. Control mice received the same intraperitoneal volume of saline. After 30-min pretreatment, animals were injected with 20 μL 0.92% (vol/vol) formalin at the plantar surface of right hind paw. Mice were then placed individually into open polyvinyl cages (20 × 40 × 15 cm). The time spent licking the injected paw was recorded by digital video camera during phase I (0–5 min postinjection) and phase II (15–30 min postinjection).

Thermal Pain Test. A photothermal pain detector (YLS-12A; Jinan) was used to measure the pain threshold of mice subjected to intense heat (34). The light beam of the detector was focused on the middle portion of the tail, and mice measured to have a tail withdrawal latency of 4–6 s were selected for

the tail-flick test. Test animals were injected intraperitoneally with 100 μL saline containing Ssm6a or morphine 30 min before photothermal heating of the tail. The control group received the same volume of saline. Tail withdrawal latency was measured as the time taken to withdraw the tail from the light beam.

Abdominal Writhing Induced by Acetic Acid. Mice were injected intraperitoneally with 100 μL saline containing Ssm6a or morphine 30 min before intraperitoneal injection of 200 μL 0.8% (vol/vol) acetic acid, which induces abdominal contractions and hind limb stretching (35). The control group received the same volume of saline. Mice were placed into open polyvinyl cages (20 × 40 × 15 cm) immediately after acid challenge, and abdominal constrictions were counted cumulatively over a period of 30 min.

Recombinant Peptide Production. Recombinant Ssm6a was produced via expression in the periplasm of *Escherichia coli* as described for the spider-venom peptide PcTx1 (36). Further details are provided in *SI Materials and Methods* (Fig. S8). Note that native toxin was used for all electrophysiological and animal studies.

Plasma Stability. Lyophilized human plasma (Sigma-Aldrich, batch 101M7025) was resuspended in an equivalent volume of ultrapure water, then lyophilized recombinant Ssm6a or rat atrial natriuretic peptide (American Peptide Company, Cat. No. 14–5-41) was added to a final concentration of 20 μM and samples were incubated at 37 °C for 7 d. Triplicate samples were taken at selected time points, quenched by addition of urea, then plasma proteins were precipitated with 20% (vol/vol) trichloroacetic acid. Samples were centrifuged at 14,900 × *g* for 15 min, then supernatants were fractionated via C_{18} RP-HPLC. The peak corresponding to intact Ssm6a was identified by coelution with native toxin and mass determination via MALDI-TOF mass spectrometry using α-cyano-4-hydroxycinnamic acid matrix on a 4700 Proteomics Bioanalyzer (Applied Biosystems). Ssm6a levels were then quantified from peak absorbance at 214 nm.

CD Spectropolarimetry. CD spectra of Ssm6a (20 μM in 10 mM $KHPO_4$, pH 7.2) were acquired at 20 °C under constant N_2 flush using a Jasco J-810 spectropolarimeter. Spectra were the sum of eight scans acquired over the region 260–190 nm at 20 nm/min. Percent helicity was determined from the mean residue ellipticity at 222 nm (θ_{222}), as described previously (37).

Thermal denaturation profiles were obtained by monitoring θ_{222} as the temperature was increased from 20 to 95 °C at a rate of 2 °C/min. Denaturation curves were fitted with a six parameter sigmoidal function (38) to obtain T_m values. The thermal denaturation of Ssm6a was completely reversible upon cooling.

ACKNOWLEDGMENTS. We thank Prof. Jamie Vandenberg for kindly providing the hERG clone, Ho Yee Lau for recombinant VSTX1 peptide, and Dr. Yucheng Xiao for help with data analysis. This study was supported by the Chinese National Natural Science Foundation (30830021, 31025025, 31070701, 31000960, 31025025, U1132601, 31200590), the Chinese Ministry of Science and Technology (2010CB529800, 2011ZX09102-002-10), Yunnan Province (2011CI139, 2012BC009), and the Australian Research Council (Discovery Grant DP110103129).

1. Brennan F, Carr DB, Cousins M (2007) Pain management: A fundamental human right. *Anesth Analg* 105(1):205–221.
2. Gaskin DJ, Richard P (2012) The economic costs of pain in the United States. *J Pain* 13(8):715–724.
3. Payandeh J, Scheuer T, Zheng N, Catterall WA (2011) The crystal structure of a voltage-gated sodium channel. *Nature* 475(7356):353–358.
4. Basbaum AI, Bautista DM, Scherrer G, Julius D (2009) Cellular and molecular mechanisms of pain. *Cell* 139(2):267–284.
5. Yu FH, Catterall WA (2003) Overview of the voltage-gated sodium channel family. *Genome Biol* 4(3):207.
6. King GF, Escoubas P, Nicholson GM (2008) Peptide toxins that selectively target insect $Na_{(V)}$ and $Ca_{(V)}$ channels. *Channels (Austin)* 2(2):100–116.
7. Dib-Hajj SD, Yang Y, Black JA, Waxman SG (2013) The $Na_{(V)}1.7$ sodium channel: From molecule to man. *Nat Rev Neurosci* 14(1):49–62.
8. Cox JJ, et al. (2006) An *SCN9A* channelopathy causes congenital inability to experience pain. *Nature* 444(7121):894–898.
9. Minett MS, et al. (2012) Distinct Nav1.7-dependent pain sensations require different sets of sensory and sympathetic neurons. *Nat Commun* 3:791.
10. Reimann F, et al. (2010) Pain perception is altered by a nucleotide polymorphism in *SCN9A*. *Proc Natl Acad Sci USA* 107(11):5148–5153.
11. Weiss J, et al. (2011) Loss-of-function mutations in sodium channel Nav1.7 cause anosmia. *Nature* 472(7342):186–190.
12. Rupasinghe DB, et al. (2012) Localization of Na_v 1.7 in the normal and injured rodent olfactory system indicates a critical role in olfaction, pheromone sensing and immune function. *Channels (Austin)* 6(2):103–110.
13. Undheim EA, King GF (2011) On the venom system of centipedes (Chilopoda), a neglected group of venomous animals. *Toxicon* 57(4):512–524.
14. Yang S, et al. (2012) Chemical punch packed in venoms makes centipedes excellent predators. *Mol Cell Proteomics* 11(9):640–650.
15. Mobli M, King GF (2010) NMR methods for determining disulfide-bond connectivities. *Toxicon* 56(6):849–854.
16. Black JA, Frézel N, Dib-Hajj SD, Waxman SG (2012) Expression of Nav1.7 in DRG neurons extends from peripheral terminals in the skin to central preterminal branches and terminals in the dorsal horn. *Mol Pain* 8:82.
17. Chen J, et al. (2009) Expression and characterization of jingzhaotoxin-34, a novel neurotoxin from the venom of the tarantula *Chilobrachys jingzhao*. *Peptides* 30(6):1042–1048.
18. Bosmans F, et al. (2006) Four novel tarantula toxins as selective modulators of voltage-gated sodium channel subtypes. *Mol Pharmacol* 69(2):419–429.
19. Bosmans F, Martin-Eauclaire MF, Swartz KJ (2008) Deconstructing voltage sensor function and pharmacology in sodium channels. *Nature* 456(7219):202–208.
20. McNamara CR, et al. (2007) TRPA1 mediates formalin-induced pain. *Proc Natl Acad Sci USA* 104(33):13525–13530.
21. King GF (2011) Venoms as a platform for human drugs: Translating toxins into therapeutics. *Expert Opin Biol Ther* 11(11):1469–1484.
22. Ahmad S, et al. (2007) A stop codon mutation in *SCN9A* causes lack of pain sensation. *Hum Mol Genet* 16(17):2114–2121.
23. Goldberg YP, et al. (2007) Loss-of-function mutations in the $Na_v1.7$ gene underlie congenital indifference to pain in multiple human populations. *Clin Genet* 71(4):311–319.
24. Yang Y, et al. (2004) Mutations in *SCN9A*, encoding a sodium channel alpha subunit, in patients with primary erythermalgia. *J Med Genet* 41(3):171–174.
25. England S, de Groot MJ (2009) Subtype-selective targeting of voltage-gated sodium channels. *Br J Pharmacol* 158(6):1413–1425.
26. Caldwell JH, Schaller KL, Lasher RS, Peles E, Levinson SR (2000) Sodium channel $Na_{(v)}1.6$ is localized at nodes of ranvier, dendrites, and synapses. *Proc Natl Acad Sci USA* 97(10):5616–5620.
27. Klint JK, et al. (2012) Spider-venom peptides that target voltage-gated sodium channels: Pharmacological tools and potential therapeutic leads. *Toxicon* 60(4):478–491.
28. Schmalhofer WA, et al. (2008) ProTx-II, a selective inhibitor of $Na_V1.7$ sodium channels, blocks action potential propagation in nociceptors. *Mol Pharmacol* 74(5):1476–1484.
29. Clare JJ (2010) Targeting voltage-gated sodium channels for pain therapy. *Expert Opin Investig Drugs* 19(1):45–62.
30. King GF, Hardy MC (2013) Spider-venom peptides: Structure, pharmacology, and potential for control of insect pests. *Annu Rev Entomol* 58:475–496.
31. Xiao Y, et al. (2004) Jingzhaotoxin-III, a novel spider toxin inhibiting activation of voltage-gated sodium channel in rat cardiac myocytes. *J Biol Chem* 279(25):26220–26226.
32. Beacham D, Ahn M, Catterall WA, Scheuer T (2007) Sites and molecular mechanisms of modulation of $Na_{(v)}1.2$ channels by Fyn tyrosine kinase. *J Neurosci* 27(43):11543–11551.
33. Rong M, et al. (2011) Molecular basis of the tarantula toxin jingzhaotoxin-III (β-TRTX-Cj1α) interacting with voltage sensors in sodium channel subtype Nav1.5. *FASEB J* 25(9):3177–3185.
34. Wei L, et al. (2011) Analgesic and anti-inflammatory effects of the amphibian neurotoxin, anntoxin. *Biochimie* 93(6):995–1000.
35. Santos JA, et al. (2012) Anti-inflammatory effects and acute toxicity of hydroethanolic extract of *Jacaranda decurrens* roots in adult male rats. *J Ethnopharmacol* 144(3):802–805.
36. Saez NJ, et al. (2011) A dynamic pharmacophore drives the interaction between Psalmotoxin-1 and the putative drug target acid-sensing ion channel 1a. *Mol Pharmacol* 80(5):796–808.
37. Szeto TH, Rowland SL, Habrukowich CL, King GF (2003) The MinD membrane targeting sequence is a transplantable lipid-binding helix. *J Biol Chem* 278(41):40050–40056.
38. Bains NPS, Wilce JA, Mackay LG, King GF (1999) Controlling leucine zipper specificity with interfacial hydrophobic residues. *Lett Pept Sci* 6:381–390.
39. Klinger AB, et al. (2012) Sea-anemone toxin ATX-II elicits A-fiber-dependent pain and enhances resurgent and persistent sodium currents in large sensory neurons. *Mol Pain* 8:69.
40. Wilson MJ, et al. (2011) μ-Conotoxins that differentially block sodium channels $Na_V1.1$ through 1.8 identify those responsible for action potentials in sciatic nerve. *Proc Natl Acad Sci USA* 108(25):10302–10307.